CrossMark

ORIGINAL INVESTIGATION

Mutation of the mitochondrial carrier SLC25A42 causes a novel form of mitochondrial myopathy in humans

Hanan E. Shamseldin[1] · Laura L. Smith[2] · Amal Kentab[3] · Hisham Alkhalidi[4] ·
Brady Summers[5] · Haifa Alsedairy[1] · Yong Xiong[5] · Vandana A. Gupta[2] ·
Fowzan S. Alkuraya[1,6]

Abstract Myopathies are heterogeneous disorders characterized clinically by weakness and hypotonia, usually in the absence of gross dystrophic changes. Mitochondrial dysfunction is a frequent cause of myopathy. We report a simplex case born to consanguineous parents who presented with muscle weakness, lactic acidosis, and muscle changes suggestive of mitochondrial dysfunction. Combined autozygome and exome analysis revealed a missense variant in the *SLC25A42* gene, which encodes an inner mitochondrial membrane protein that imports coenzyme A into the mitochondrial matrix. Zebrafish *slc25a42* knockdown morphants display severe muscle disorganization and weakness. Importantly, these features are rescued by normal human *SLC25A42* RNA, but not by RNA harboring the patient's variant. Our data support a potentially causal link between *SLC25A42* mutation and mitochondrial myopathy in humans.

H. E. Shamseldin and L. L. Smith have contributed equally.

Electronic supplementary material The online version of this article (doi:10.1007/s00439-015-1608-8) contains supplementary material, which is available to authorized users.

✉ Vandana A. Gupta
vgupta@enders.tch.harvard.edu

✉ Fowzan S. Alkuraya
falkuraya@kfshrc.edu.sa

1 Department of Genetics, King Faisal Specialist Hospital and Research Center, Riyadh, Saudi Arabia

2 Division of Genetics and Genomics, The Manton Center for Orphan Disease Research, Harvard Medical School, Boston Children's Hospital, Boston, MA, USA

3 Department of Pediatrics, College of Medicine, King Saud University, Riyadh, Saudi Arabia

4 Department of Pathology, College of Medicine, King Saud University, Riyadh, Saudi Arabia

5 Department of Molecular Biophysics and Biochemistry, Yale University, New Haven, CT, USA

6 Department of Anatomy and Cell Biology, College of Medicine, Alfaisal University, Riyadh, Saudi Arabia

Introduction

Mitochondria are membrane-bound organelles that are ubiquitous in eukaryotes and house the molecular machinery necessary for oxidative phosphorylation (oxphos), the main source of ATP-related energy production (Lang et al. 1999). Defects in oxphos result in energy-deficient states that are highly variable in their clinical presentation, depending on the severity of the defect and its tissue distribution (Fernández-Vizarra et al. 2009). In the case of oxphos-related mitochondrial-DNA (m-DNA) mutations, differential expression between or within tissues is often an effect of mutation load. However, despite an equal mutation load across tissues, nuclear-DNA (n-DNA) mutations involving genes critical for oxphos function can also have remarkably variable tissue distributions (Smeitink et al. 2001).

Myopathy, which manifests clinically as muscle weakness without gross dystrophic changes, is a very common phenotype in oxphos disorders and is usually attributed to the high energy demand of contractile muscle tissue. Mitochondrial myopathies can have significant overlap with other genetic forms of myopathy, but can be differentiated on the basis of clinical and laboratory features (Bernier et al. 2002; Haas et al. 2007, 2008; Wolf and Smeitink 2002). Affected individuals frequently present with encephalopathy, as the brain is another tissue requiring vast

amounts of energy. Resting lactic acidosis is another highly suggestive feature of oxphos disorders, due to impairments in cellular respiration and perturbations in the cytoplasmic $NADH:NAD^+$ ratio (Debray et al. 2007). While histopathological and direct assays of oxphos on muscle tissues can also help to assign diagnosis, identification of the causal mutation is the preferred and most informative diagnostic method.

Most mitochondrial myopathies are caused by mutations in n-DNA. Such mutations in more than 200 genes have been reported to date, and hundreds more are now considered likely candidates based on their established role in mitochondrial physiology (Chen 2015; Milone and Wong 2013). Affected genes are not limited to those encoding individual components of the electron transport chain, but also include those coding for a wide array of factors responsible for maintaining mitochondrial homeostasis (e.g., mitochondrial polymerases, helicases, aminoacyl t-RNA transferases) (Chen 2015; Milone and Wong 2013). One major challenge in the molecular diagnosis of mitochondrial myopathies is the lack of helpful clinical and laboratory markers to guide mutation analysis. However, the advent of genomic sequencing tools that are agnostic to the clinical presentation has markedly accelerated the discovery of novel genes that are mutated in these disorders. This is especially true when these techniques are combined with autozygosity in consanguineous populations (Calvo et al. 2012; Gai et al. 2013; Shamseldin et al. 2012; Vasta et al. 2009). As part of our ongoing effort to characterize novel causes of mitochondrial disorders in the highly consanguineous population of Saudi Arabia (Alkuraya 2014), we describe the identification of *SLC25A42* as a novel candidate gene with supporting evidence from the zebrafish model.

Materials and methods

Human subjects

Patient was evaluated by a board-certified clinical geneticist and pediatric neurologist, each with expertise in mitochondrial disorders. Informed consent was obtained as per KFSHRC IRB-approved research protocol (RAC #2121053). Venous blood was collected from index and available family members in EDTA tubes for DNA extraction.

Autozygome analysis

Mapping of the entire set of autozygous intervals in the index genome (autozygome) was performed as previously described (Alkuraya 2012). Briefly, runs of homozygosity >2 Mb in size were taken as surrogates of autozygosity and

were determined genome wide using AutoSNPa analysis of SNP genotypes generated by the Axiom SNP Chip platform (Affymetrix, Santa Clara, CA, USA).

Exome sequencing and variant filtering

Exome capture was performed using the TruSeq Exome Enrichment kit (Illumina, San Diego, CA, USA) as per the manufacturer's instructions. Samples were prepared as an Illumina sequencing library, and in the second step, the sequencing libraries were enriched for the desired target using the Illumina Exome Enrichment protocol. Captured libraries were sequenced using the Illumina HiSeq 2000 Sequencer, and the reads mapped against UCSC hg19 (http://genome.ucsc.edu/) by BWA (http://bio-bwa.source-forge.net/). The SNPs and Indels were detected by SAMTOOLS (http://samtools.sourceforge.net/). The resulting variants were filtered as follows: homozygous => coding/splicing => within autozygome of the index => absent or very rare in Saudi and public exome databases => predicted to be pathogenic by SIFT/PolyPhen/CADD, as previously described (Alkuraya 2013).

Zebrafish husbandry

Zebrafish (*Danio rerio*) from the wild-type Oregon AB line were bred and maintained according to standard procedures in the Boston Children's Hospital aquatic research program facility (Westerfield 2007). Embryos were collected by natural spawning, staged by hours (hpf) or days (dpf) post-fertilization (Kimmel et al. 1995), and raised at 28.5 °C in egg water. All animal work was performed with approval from the Boston Children's Hospital Animal Care and Use Committee (14-05-2717R).

Morpholino knockdown and mRNA rescue

Two antisense morpholinos (MOs), one targeting the translational start site (T-MO) and one targeting the exon 3-intron3 splice site (e3i3-MO), were designed to knockdown the zebrafish *slc25a42* transcript (NM_001045453.1; GeneTools LLC, Philomath, OR, USA). The morpholino sequences were *slc25a42* T-MO: 5′-CTTCCTTCACAC CATTACCCATACC-3′ and *slc25a42* e3i3-MO: 5′-GGC CAACACTTACCTTGGAAGATGA-3′. A morpholino against human β-globin, which is not homologous to any sequence in the zebrafish genome by BLAST search, was used as a negative control for all injections (5′-CCTCT TACCTCAGTTACAATTTATA-3′). Morpholinos were dissolved in sterile water with 0.1 % phenol red and 1–2 nL (1–10 ng) injected into the yolk of 1-cell stage wild-type embryos. For rescue experiments, full-length human *SLC25A42* (NM_178526.4) cDNA was obtained from

the DNA Resource Core at Harvard Medical School (ID #HsCD00378128) and cloned into a pCSDest destination vector (created by Nathan Lawson) using Gateway technology (Invitrogen, Carlsbad, CA, USA). Mutant cDNA was created by incorporating the p.N291D (c.A871G) substitution into wild-type *SLC25A42* cDNA using GENEART site-directed mutagenesis (Invitrogen). This substitution was confirmed using the following sequencing primers: 5′-AAAGGCTTGAGCATGGACTGGGTCAAGGGTC-3′ (forward) and 5′-GACCCTTGACCCAGTCCATGCTCA AGCCTTT-3′ (reverse). mRNA for wild-type and mutant constructs was synthesized in vitro using mMessage mMachine SP6 kits (Ambion, Austin, TX, USA). mRNAs (100–200 pg) were injected into embryos at the 1-cell stage independently or in combination with T-MO, and subsequent phenotypic analyses performed at 3 dpf.

Western blotting

Zebrafish embryos at 3 dpf were homogenized in buffer containing Tris–Cl (20 mM, pH 7.6), NaCl (50 mM), EDTA (1 mM), NP-40 (0.1 %) and complete protease inhibitor cocktail (Roche Applied Sciences, Indianapolis, IN, USA). Following centrifugation at 11,000g at 4 °C for 15 min, protein concentration in supernatants was determined by BCA protein assay (Pierce, Rockford, IL, USA). Proteins were separated by electrophoresis on 4–12 % gradient Tris–glycine gels (Invitrogen) and transferred onto polyvinylidene difluoride membrane (Invitrogen). Membranes were blocked in PBS containing 5 % casein and 0.1 % Tween-20, then incubated with either mouse polyclonal anti-SLC25A42 (1:500, ab69383, Abcam, Cambridge, MA, USA) or mouse monoclonal anti-β-actin (1:1000, A5441, Sigma, St. Louis, MO) primary antibodies. After washing, membranes were incubated with horseradish peroxidase-conjugated anti-mouse (1:5000, 170-6516) IgG secondary antibody (BioRad, Hercules, CA, USA). Proteins were detected using the SuperSignal chemiluminescent substrate kit (Pierce).

Histopathology

For electron microscopy, 3 dpf zebrafish embryos were fixed in formaldehyde–glutaraldehyde–picric acid in cacodylate buffer overnight at 4 °C, followed by osmication and uranyl acetate staining. Subsequently, embryos were dehydrated in a series of ethanol washes and embedded in TAAB Epon (Marivac Ltd., Halifax, Nova Scotia, Canada). Sections (95 nm) were cut with a Leica UltraCut microtome, picked up on 100-μm Formvar-coated copper grids, and stained with 0.2 % lead citrate. Sections were viewed and imaged under a Philips Tecnai BioTwin Spirit electron microscope (Philips, Amsterdam, The Netherlands) at the Harvard Medical School Electron Microscopy Core.

Whole-mount immunofluorescence

Whole-mount phalloidin staining for filamentous actin was performed on 3 dpf embryos as described previously (Gupta et al. 2013). Briefly, embryos were fixed in 4 % PFA overnight at 4 °C, then washed as follows: 2 × 10 min in PBS, 2 × 10 min in PBS-T (0.1 % Tween-20), 1 × 60 min in PBS-TR (2 % Triton X), and 2 × 5 min in PBS-T. Embryos were blocked in PBS-T containing 5 % goat serum for 1 h at RT, and incubated with Alexa Fluor® 488 phalloidin (1:20, A12379, Invitrogen) overnight at 4 °C. Embryos were washed 4 × 15 min in PBS-T before being mounted in 70 % glycerol and visualized using a Perkin Elmer UltraVIEW VoX spinning disk confocal microscope.

Statistical analysis

Data were statistically analyzed by parametric Student's t test (two-tailed) and were considered significant when $P < 0.01$. All data analyses were performed using GraphPad Prism 6 software (GraphPad Software Inc., La Jolla, CA, USA) and are described as the mean ± standard deviation.

Results

Clinical report

The patient (index, III-6) is a 16-year-old Saudi boy born at 37 weeks to a gravida 5, para 2, 4 abortion mother via cesarean section with a birth weight of 2.2 kg (other growth parameters are unavailable). His parents are consanguineous, and the family history is significant for recurrent miscarriages (Fig. 1). There were no reported neonatal complications. Developmental history was remarkable for motor delays: he only sat at 24 months and walked independently by his third birthday. He is currently in the tenth grade and doing well academically. While he complains of frequent muscle aches after muscle use, there is no history of urine discoloration. His medical history is also notable for mild scoliosis and non-progressive myopia.

He was first brought to medical attention for frequent falling and fatigue after walking at the age of 3 years. There is no evidence of progression and he continues to be mobile at 16 years of age, although he is unable to run. Other functional limitations caused by his muscle weakness include limited physical activity due to chronic fatigue, inability to carry heavy objects and dysarthria. On examination, he was noted to have normal growth parameters (height on

Fig. 1 Human data. **a** Pedigree of the study family. Histopathological findings on the index's muscle biopsy. **b** Hematoxylin and eosin stain indicates myopathy, with moderate variation of fiber size and scattered atrophic/hypertrophic fibers. **c** Cytochrome c oxidase (COX) staining: COX levels are reduced in scattered muscle fibers (*double arrows*). Other fibers show subsarcolemmal mitochondrial accumulation (*single arrow*). **d** Succinic dehydrogenase (SDH) staining: scattered muscle fibers with mitochondrial proliferation stain darkly for SDH. **e** Trichrome staining: ragged *red* muscle fibers are detected. These cells have mild to moderate mitochondrial proliferation as revealed by Gomori trichrome stain. The sarcoplasm has a *red* rim and speckled appearance
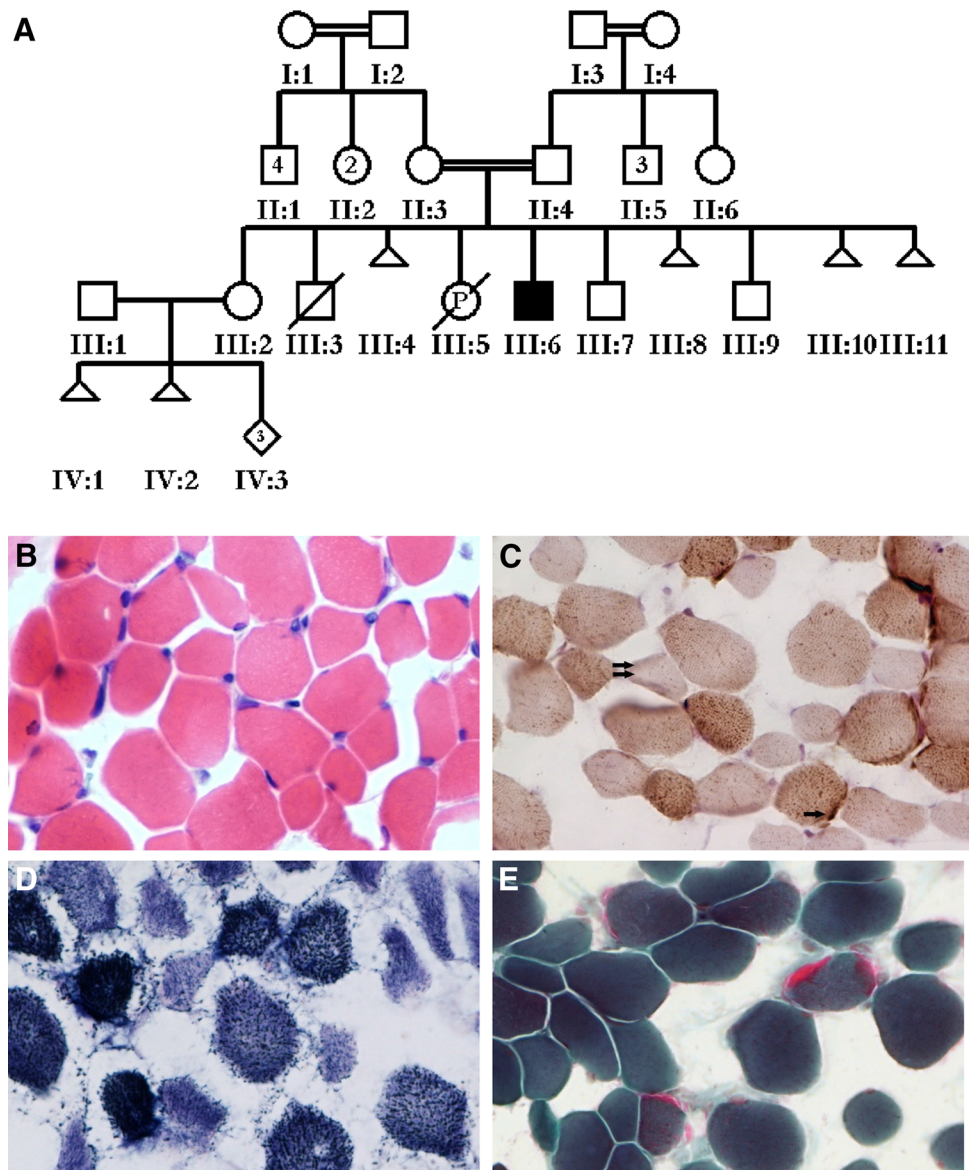

25th percentile, and weight on 10th percentile with normal growth velocity), mild dysarthria, facial muscle weakness, poor muscle mass, and mild, mostly proximal muscle weakness (4/5 power). His tone and deep tendon reflexes were normal and there was no evidence of extraocular muscle involvement or optic atrophy.

His workup included elevated levels of lactic acid (primary lactic acidosis ranging 4.2–8.7 mmol/L, normal range is 1.5–2.2 mmol/L). Spine X-ray revealed spondylolisthesis at L5–S1 with right lumbar curve scoliosis of 13° noted at T12–L3. Creatine kinase level, nerve conduction studies, brain MRI and CT, and echocardiography were all within normal limits. Muscle biopsy revealed ragged red-like fibers with enhanced subsarcolemmal oxidative enzyme activity, and other fibers showing markedly decreased cytochrome c oxidase (COX) activity (Fig. 1).

SLC25A42 is mutated in a patient with mitochondrial myopathy

The index's typical clinical presentation for mitochondrial myopathy prompted combined autozygome/exome analysis, a previously described strategy that exploits the consanguineous nature of families (Alkuraya 2013). As shown in Fig. 2, the initial list of 71,614 exomic variants were iteratively filtered to a single variant by applying the following filters: homozygosity, within autozygome, novel or very rare (MAF <0.001) and in silico prediction of pathogenicity. The single remaining variant was *SLC25A42*:NM_178526:c.871A > G:p.N291D. This missense variant was only homozygous in the index; parents were heterozygous and his unaffected siblings were either heterozygous (III:2) or wild-type (III:7 and III:9). This
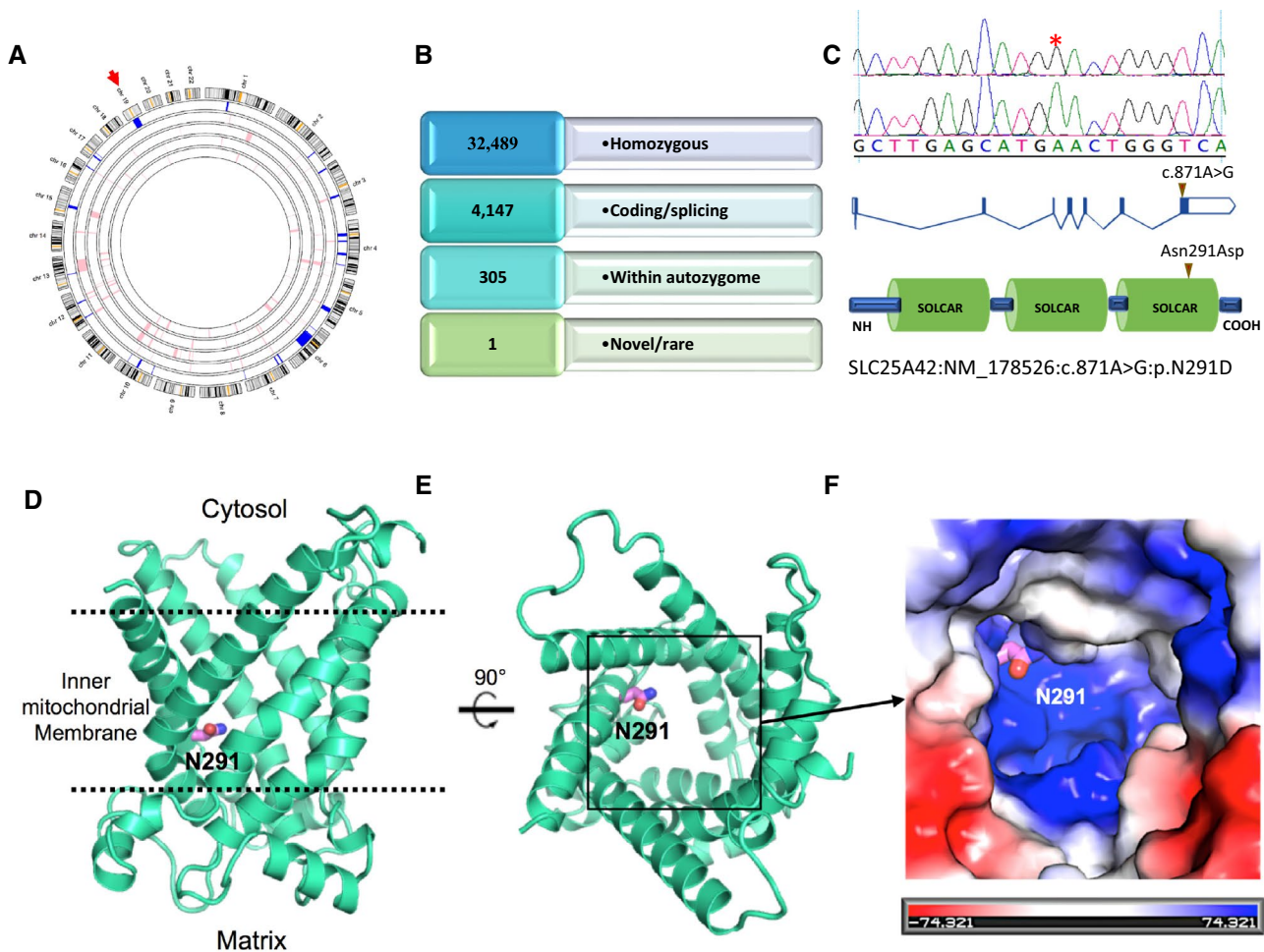
Fig. 2 Identification of a novel *SLC25A42* variant in a patient with mitochondrial myopathy. **a** Autozygome analysis is shown genome-wide. Autozygous intervals are depicted as blue bars in the outer circle representing the index (the *inner four circles* represent the parents and siblings). **b** Filtering scheme of exome variants. **c** Cartoon of SLC25A42 gene and protein and the location of the mutation is indicated by *red triangles*. Homology model of the SLC25A42 protein showing the proximity of N291 to the positively charged substrate-binding site, based on the crystal structures of ADP/ATP transporters (PDB IDs: 1OKC, 4C9Q) and the mitochondrial uncoupling protein (PDB ID: 2LCK). **d** The SLC25A42 model structure in cartoon repre-

sentation (*green cyan*) with N291 in stick representation (*violet/blue*). The membrane boundaries are represented by *dashed lines* (*black*). **e** View of the SLC25A42 substrate-binding groove from the cytosolic side of the membrane. N291 is oriented towards the substrate-binding site. **f** Surface representation of the positively charged substrate-binding site of SLC25A42 (*boxed* region in B) with the surface colored according to electrostatic potentials (*blue* positive, *red* negative, unit KbT/ec). N291 is adjacent to a basic patch that is likely important for the binding of negatively charged phosphate group. An N291D mutation may disfavor binding of negatively charged groups or affect the efficient transport of the substrate

variant was also absent in our in-house database of ~700 exomes, as well as the ExAC Browser. All three in silico prediction tools used to assess pathogenicity assigned a high likelihood of pathogenicity (PolyPhen 1, SIFT 0.00, and CADD 29.4). As shown in Figure S1, the involved residue is conserved across all known orthologs.

The SLC25A42 protein is a mitochondrial coenzyme A transporter, which is an integral membrane protein found in the inner mitochondrial membrane (Fiermonte et al. 2009). It is a member of the conserved mitochondrial carrier family of proteins that transport a variety of substrates between the cytosol and mitochondrial matrix

(see (Palmieri 2004) for review). Members of this family have a highly conserved domain architecture consisting of three tandem sequence repeats (Saraste and Walker 1982), with each repeat containing two transmembrane helices and a conserved PX(D/E)XX(K/R) motif that is the signature of the protein family (Nelson et al. 1998). The six combined transmembrane helices are oriented with threefold pseudo-symmetry and create a deep groove in the membrane that contains the substrate-binding site (Berardi et al. 2011; Pebay-Peyroula et al. 2003; Ruprecht et al. 2014). Large conformational changes are predicted to occur to allow transport, although the mechanism is

poorly understood (see (Palmieri and Pierri 2010) for review).

There are three unique structures of members of this family deposited in the Protein Data Bank—the bovine ADP/ATP carrier (Pebay-Peyroula et al. 2003), the yeast ADP/ATP carrier (Ruprecht et al. 2014), and the mouse mitochondrial uncoupling protein (Berardi et al. 2011). The homology modeling engine *Phyre2* modeled the structure of SLC25A42 with greater than 90 % confidence, using deposited PDB structures as templates (Kelley et al. 2015) (PDB IDs: 1OKC, 4C9Q, 2LCK). The modeled structure displayed the highly conserved features of the mitochondrial carrier family (Fig. 2d, e).

The predicted substrate-binding site of SLC25A42 shares a high degree of homology to the binding site of bovine and yeast ADP/ATP carriers likely due to structural similarities between coenzyme A and ADP (Robinson et al. 2008). Indeed, it has been shown that SLC25A42 is capable of efficiently transporting ADP in addition to coenzyme A and other substrates (Fiermonte et al. 2009). The substrate-binding region of SLC25A42 is predicted to be highly positively charged like that of the ADP/ATP transporters, and these positively charged regions are likely to be involved in binding of phosphate moieties (Fig. 2f) (Robinson et al. 2008). Several amino acids of SLC25A42 are predicted to interact with the adenine base and phosphate groups of coenzyme A, and homologous amino acids in ADP/ATP transporters have been demonstrated biochemically to be important in ADP binding (Dehez et al. 2008; Robinson and Kunji 2006; Robinson et al. 2008; Wang and Tajkhorshid 2008).

N291 is conserved between SLC25A42 and both bovine and yeast ADP/ATP carriers. It faces the interior of the substrate-binding groove (Fig. 2d, e). Its proximity to several positively charged amino acids predicted to be important in phosphate binding may be critical in explaining the detrimental effect of the N291D mutation. A negatively charged aspartate in this position may disfavor the binding of negatively charged phosphate groups, thus inhibiting coenzyme A binding and transport. Due to its important location in the substrate-transporting channel, it is also possible that the N291D mutation inhibits the interaction with other moieties of the substrate, or affects the structural/biochemical properties of the transporter that are required for efficient substrate exchange.

## Slc25a42 deficiency causes a severe muscle phenotype not rescued by N291D-encoding human *SLC25A42* mRNA

An Slc25a42-deficient zebrafish model was constructed using two antisense MOs complementary to the zebrafish *slc25a42* gene (NM_178526.4) (Fig. 3a–c). Quantification

of Western blot analyses confirmed reduced levels of endogenous zebrafish Slc25a42 protein in morphant embryos injected with translation-blocking MO by 3 dpf (Fig. 3d), whereas splice-blocking MO injections targeting the exon 3-intron 3 boundary resulted in a truncated, presumably non-functional form of the protein with a lower molecular weight (Fig. 3e). Both MOs independently yielded one specific zebrafish phenotype, with morphological anomalies including dorsal curvature and bent tails, as well as evidence of early motor defects. While healthy developing zebrafish embryos typically hatch from their protective chorions by 2–2.5 dpf, MO-injected zebrafish morphants remained in their chorion until 3–3.5 dpf and required manual dechorionation for imaging. Importantly, full-length human wild-type *SLC25A42* mRNA was able to significantly rescue the physical traits and motor deficiencies of *slc25a42* zebrafish morphants, represented by the 70.5 ± 8.0 % of rescued embryos hatched from the chorion by 3 dpf ($P < 0.01$). However, overexpression of human *SLC25A42* mRNA encoding the p.N291D (c.A871G) missense mutation in exon 8 was not able to restore the wild-type phenotype or hatching rate to *slc25a42* zebrafish morphants. Mutant mRNA rescues showed only 13.3 ± 6.2 % of timely hatched embryos, similar to the 8.1 ± 2.6 % of hatched embryos observed in clutches injected with MO alone by 3 dpf ($P > 0.05$) (Fig. 3f).

To investigate the potential cause of morphant skeletal muscle weakness at the cellular level, we performed non-invasive birefringence assays (Smith et al. 2013), followed by whole-mount immunofluorescence staining for filamentous actin. Both sets of experiments suggested that MO-injected morphant muscles are overall organized and structured similar to wild-type controls (Figure S2). Subsequent analyses of electron micrographs, however, revealed substantial abnormalities specific to mitochondria (Fig. 4a–d). In particular, the inner mitochondrial membrane in morphant embryos was fragmented into smaller size vesicles, lacking the dense membranous network seen in control mitochondria. Together, our results confirm that loss of *SLC25A42* gene function may be involved in the disease pathogenesis of a mitochondrial myopathy and implicate a novel human missense mutation in this role.

Discussion

SLC25 is the largest family of solute carrier proteins and includes members encoded by over 50 human genes (Palmieri 2013). Nearly, all SLC25 proteins localize to the mitochondria, where they facilitate metabolic communication between the cytosol and the matrix, although few are also known to localize to other organelle membranes. Despite their relatedness, however, the several human diseases
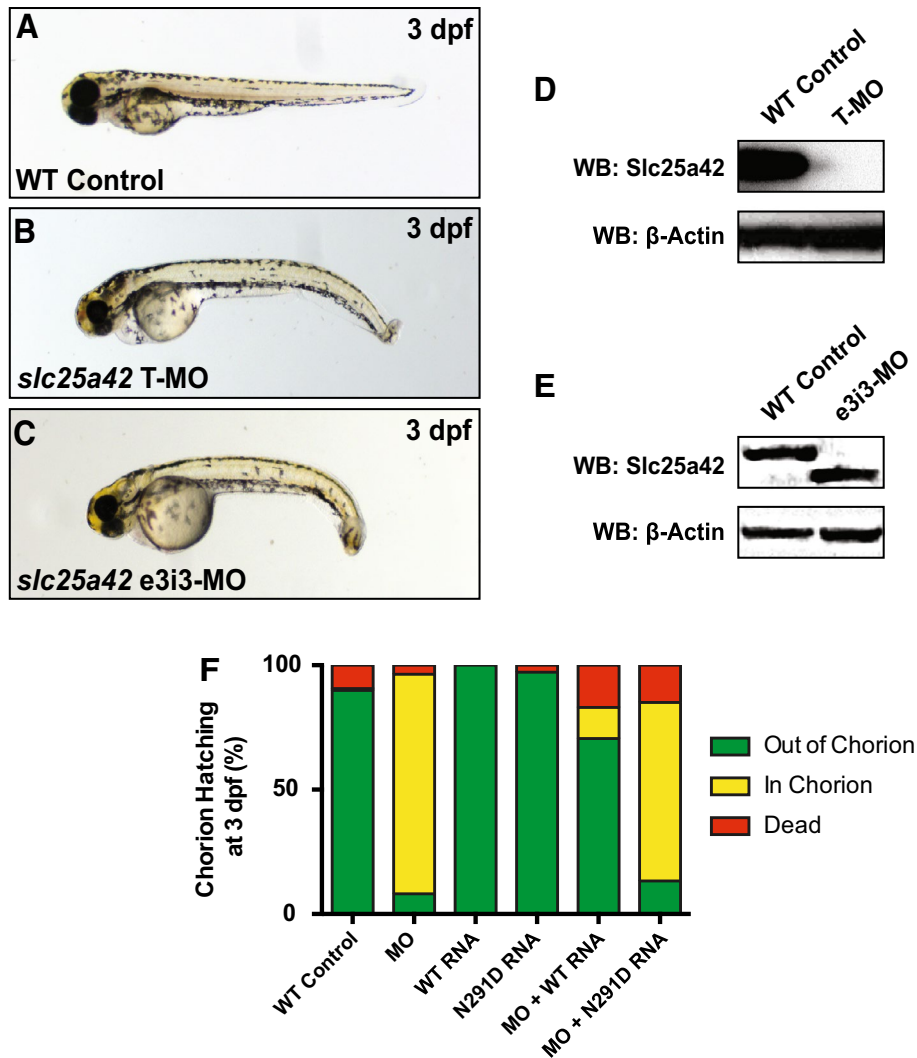
Fig. 3 *Slc25a42* gene knockdown results in morphological defects in zebrafish. **a** Wild-type control zebrafish at 3 dpf. **b**, **c** Representative zebrafish embryos injected with 10 ng of *slc25a42* translation- (T-MO) and splice-blocking (e3i3-MO) morpholinos both show dorsally curved and mildly hypotonic phenotypes at 3 dpf. **d**, **e** Western blot demonstrates that T- and e3i3-MO-mediated knockdowns of *slc25a42* result in significantly decreased levels of zebrafish Slc25a42 protein or a truncated form of the protein, respectively, by 3 dpf. Polyclonal antibody directed against the full-length human SLC25A42 protein (NP_848621.2) was used for detection. β-Actin was used as a loading control. **f** Quantification of chorion hatching rates observed with mRNA overexpression in wild-type and *slc25a42* morphants (WT: 89.9 ± 5.3 % hatched; MO: 8.1 ± 2.6 % hatched; WT RNA: 100.0 ± 0.0 % hatched; N291D RNA: 97.2 ± 2.8 % hatched; MO + WT RNA: 70.5 ± 8.0 % hatched; MO + N291D RNA: 13.3 ± 6.2 % hatched). *Green* indicates normal embryos, *yellow* indicates morphant embryos, and *red* indicates dead embryos at 3 dpf. Wild-type embryos injected with mRNA only (no MO), as well as those injected with a negative control MO targeting the human β-globin gene, are included as controls. Two independent experiments were performed for all rescue studies, with at least 100 embryos injected for each group. Statistical significance relative to the MO-only experimental group was determined by a Student's *t* test, *P* < 0.01

resulting from Mendelian mutations in individual members suggest that many have non-redundant, discrete functions. For example, mutations in *SLC25A13*, *SLC25A15*, *SLC25A19*, *SLC25A20*, *SLC25A22*, and *SLC25A38* cause citrullinemia type II, hyperornithinemia–hyperammonemia–homocitrullinuria (HHH) syndrome, Amish microcephaly, carnitine/acylcarnitine carrier deficiency, early epileptic encephalopathy and sideroblastic anemia, respectively (Camacho et al. 1999; Guernsey et al. 2009; Huizing

et al. 1997; Kobayashi et al. 1999; Molinari et al. 2005; Rosenberg et al. 2002). More relevant to the phenotype we describe here is the *SLC25A4*-related AAC1 deficiency, which manifests as severe myopathy with extraocular muscle involvement (Kaukonen et al. 2000).

SLC25A42 is the only known mitochondrial coenzyme A (CoA) transporter (Fiermonte et al. 2009; Zallot et al. 2013). CoA plays a critical role in a myriad of reactions that take place in the mitochondrial matrix, including the
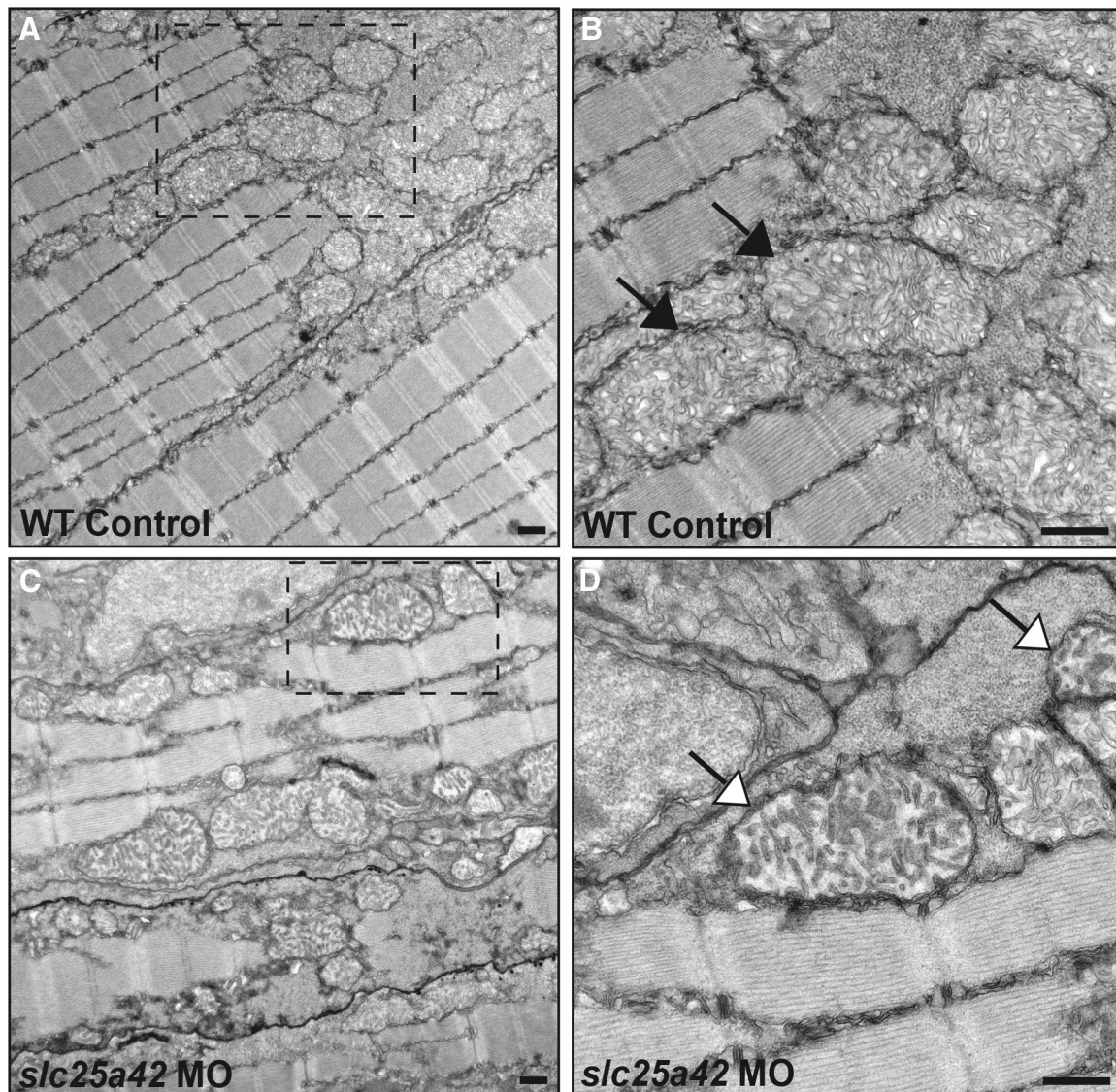
Fig. 4 Slc25a42 deficiency causes severe abnormalities in mitochondrial ultrastructure. Longitudinal transmission electron micrographs of zebrafish skeletal muscle at 3 dpf. **a**, **b** Wild-type controls show normal mitochondria (*black arrows*). **b** is an enlarged image of *dashed box* in **a**. **c**, **d** In contrast, skeletal muscles of zebrafish injected with e3i3-MO contain mitochondria with swollen and dark inner membranes (*white arrows*). **d** is an enlarged image of *dashed box* in **c**. *Scale bars* 500 nm

energy-generating beta-oxidation of fatty acids and the Krebs cycle. Therefore, it is conceivable that the severe muscle phenotype observed in *slc25a42* zebrafish morphants is caused by its non-redundant CoA importing function in skeletal muscle tissue. However, other potential mechanisms cannot be fully ruled out, as SLC25A42 also transports dephospho-CoA, poly(A) polymerase, and (deoxy)adenine nucleotides by counter-exchange across the inner mitochondrial membrane. This is supported by the presence of structurally abnormal mitochondrial inner membrane in Slc25a42-deficient morphants. Whether the phenotype is completely or partially driven by deficient CoA import into mitochondria, the failure of the mutant protein to further rescue the morphant phenotype

strongly suggests that replacing this highly conserved amino acid residue greatly impairs a muscle-relevant function of SLC25A42. This finding is consistent with the hypothesis that our patient phenotype is caused by this mutation.

In summary, we suggest that SLC25A42 is the newest member of the SLC25 superfamily of mitochondrial transporters to be associated with a human phenotype when mutated. In this case, the phenotype is a mitochondrial myopathy that largely spares other tissues commonly involved in oxphos deficiency disorders. Reports of additional patients with mutations in this novel candidate gene in the future will help to shed more light on the phenotypic spectrum of this form of myopathy.

References

Alkuraya FS (2012) Discovery of rare homozygous mutations from studies of consanguineous pedigrees. Curr Protoc Hum Genet 6.12. 1–6.12. 13

Alkuraya FS (2013) The application of next-generation sequencing in the autozygosity mapping of human recessive diseases. Hum Genet 132:1197–1211

Alkuraya FS (2014) Genetics and genomic medicine in Saudi Arabia. Mol Genet Genom Med 2:369–378

Berardi MJ, Shih WM, Harrison SC, Chou JJ (2011) Mitochondrial uncoupling protein 2 structure determined by NMR molecular fragment searching. Nature 476:109–113. doi:10.1038/nature10257

Bernier F, Boneh A, Dennett X, Chow C, Cleary M, Thorburn D (2002) Diagnostic criteria for respiratory chain disorders in adults and children. Neurology 59:1406–1411

Calvo SE, Compton AG, Hershman SG, Lim SC, Lieber DS, Tucker EJ, Laskowski A, Garone C, Liu S, Jaffe DB (2012) Molecular diagnosis of infantile mitochondrial disease with targeted next-generation sequencing. Sci Transl Med 4:118ra10–118ra10

Camacho JA, Obie C, Biery B, Goodman BK, Hu C-A, Almashanu S, Steel G, Casey R, Lambert M, Mitchell GA (1999) Hyperornithinaemia-hyperammonaemia-homocitrullinuria syndrome is caused by mutations in a gene encoding a mitochondrial ornithine transporter. Nat Genet 22:151–158

Chen H (2015) Mitochondrial myopathies. In: Chen H (ed) Atlas of genetic diagnosis and counseling. Springer, New York, pp 1–11

Debray F-G, Mitchell GA, Allard P, Robinson BH, Hanley JA, Lambert M (2007) Diagnostic accuracy of blood lactate-to-pyruvate molar ratio in the differential diagnosis of congenital lactic acidosis. Clin Chem 53:916–921

Dehez F, Pebay-Peyroula E, Chipot C (2008) Binding of ADP in the mitochondrial ADP/ATP carrier is driven by an electrostatic funnel. J Am Chem Soc 130:12725–12733. doi:10.1021/ja8033087

Fernández-Vizarra E, Tiranti V, Zeviani M (2009) Assembly of the oxidative phosphorylation system in humans: what we have learned by studying its defects. Biochim Biophys Acta Mol (BBA) Cell Res 1793:200–211

Fiermonte G, Paradies E, Todisco S, Marobbio CM, Palmieri F (2009) A novel member of solute carrier family 25 (SLC25A42) is a transporter of coenzyme A and adenosine 3′,5′-diphosphate in human mitochondria. J Biol Chem 284:18152–18159. doi:10.1074/jbc.M109.014118

Gai X, Ghezzi D, Johnson MA, Biagosch CA, Shamseldin HE, Haack TB, Reyes A, Tsukikawa M, Sheldon CA, Srinivasan S (2013)

Mutations in FBXL4, encoding a mitochondrial protein, cause early-onset mitochondrial encephalomyopathy. Am J Hum Genet 93:482–495

Guernsey DL, Jiang H, Campagna DR, Evans SC, Ferguson M, Kellogg MD, Lachance M, Matsuoka M, Nightingale M, Rideout A (2009) Mutations in mitochondrial carrier family gene SLC25A38 cause nonsyndromic autosomal recessive congenital sideroblastic anemia. Nat Genet 41:651–653

Gupta VA, Ravenscroft G, Shaheen R, Todd EJ, Swanson LC, Shiina M, Ogata K, Hsu C, Clarke NF, Darras BT (2013) Identification of KLHL41 mutations implicates BTB-Kelch-mediated ubiquitination as an alternate pathway to myofibrillar disruption in nemaline myopathy. Am J Hum Genet 93:1108–1117

Haas RH, Parikh S, Falk MJ, Saneto RP, Wolf NI, Darin N, Cohen BH (2007) Mitochondrial disease: a practical approach for primary care physicians. Pediatrics 120:1326–1333

Haas RH, Parikh S, Falk MJ, Saneto RP, Wolf NI, Darin N, Wong L-J, Cohen BH, Naviaux RK; Committee TMMSs (2008) The in-depth evaluation of suspected mitochondrial disease. Mol Genet Metab 94:16–37

Huizing M, Iacobazzi V, Ijlst L, Savelkoul P, Ruitenbeek W, van den Heuvel L, Indiveri C, Smeitink J, Trijbels F, Wanders R (1997) Cloning of the human carnitine-acylcarnitine carrier cDNA and identification of the molecular defect in a patient. Am J Hum Genet 61:1239–1245

Kaukonen J, Juselius JK, Tiranti V, Kyttälä A, Zeviani M, Comi GP, Keränen S, Peltonen L, Suomalainen A (2000) Role of adenine nucleotide translocator 1 in mtDNA maintenance. Science 289:782–785

Kelley LA, Mezulis S, Yates CM, Wass MN, Sternberg MJ (2015) The Phyre2 web portal for protein modeling, prediction and analysis. Nat Protoc 10:845–858. doi:10.1038/nprot.2015.053

Kimmel CB, Ballard WW, Kimmel SR, Ullmann B, Schilling TF (1995) Stages of embryonic development of the zebrafish. Dev Dyn 203:253–310

Kobayashi K, Sinasac DS, Iijima M, Boright AP, Begum L, Lee JR, Yasuda T, Ikeda S, Hirano R, Terazono H (1999) The gene mutated in adult-onset type II citrullinaemia encodes a putative mitochondrial carrier protein. Nat Genet 22:159–163

Lang BF, Gray MW, Burger G (1999) Mitochondrial genome evolution and the origin of eukaryotes. Annu Rev Genet 33:351–397

Milone M, Wong L-J (2013) Diagnosis of mitochondrial myopathies. Mol Genet Metab 110:35–41

Molinari F, Raas-Rothschild A, Rio M, Fiermonte G, Encha-Razavi F, Palmieri L, Palmieri F, Ben-Neriah Z, Kadhom N, Vekemans M (2005) Impaired mitochondrial glutamate transport in autosomal recessive neonatal myoclonic epilepsy. Am J Hum Genet 76:334–339

Nelson DR, Felix CM, Swanson JM (1998) Highly conserved charge-pair networks in the mitochondrial carrier family. J Mol Biol 277:285–308. doi:10.1006/jmbi.1997.1594

Palmieri F (2004) The mitochondrial transporter family (SLC25): physiological and pathological implications. Pflugers Arch 447:689–709. doi:10.1007/s00424-003-1099-7

Palmieri F (2013) The mitochondrial transporter family SLC25: identification, properties and physiopathology. Mol Aspects Med 34:465–484

Palmieri F, Pierri CL (2010) Structure and function of mitochondrial carriers—role of the transmembrane helix P and G residues in the gating and transport mechanism. FEBS Lett 584:1931–1939. doi:10.1016/j.febslet.2009.10.063

Pebay-Peyroula E, Dahout-Gonzalez C, Kahn R, Trezeguet V, Lauquin GJ, Brandolin G (2003) Structure of mitochondrial ADP/ATP carrier in complex with carboxyatractyloside. Nature 426:39–44. doi:10.1038/nature02056

Robinson AJ, Kunji ER (2006) Mitochondrial carriers in the cytoplasmic state have a common substrate binding site. Proc Natl Acad Sci USA 103:2617–2622. doi:10.1073/pnas.0509994103

Robinson AJ, Overy C, Kunji ER (2008) The mechanism of transport by mitochondrial carriers based on analysis of symmetry. Proc Natl Acad Sci USA 105:17766–17771. doi:10.1073/pnas.0809580105

Rosenberg MJ, Agarwala R, Bouffard G, Davis J, Fiermonte G, Hilliard MS, Koch T, Kalikin LM, Makalowska I, Morton DH (2002) Mutant deoxynucleotide carrier is associated with congenital microcephaly. Nat Genet 32:175–179

Ruprecht JJ, Hellawell AM, Harding M, Crichton PG, McCoy AJ, Kunji ER (2014) Structures of yeast mitochondrial ADP/ATP carriers support a domain-based alternating-access transport mechanism. Proc Natl Acad Sci USA 111:E426–E434. doi:10.1073/pnas.1320692111

Saraste M, Walker JE (1982) Internal sequence repeats and the path of polypeptide in mitochondrial ADP/ATP translocase. FEBS Lett 144:250–254

Shamseldin HE, Alshammari M, Al-Sheddi T, Salih MA, Alkhalidi H, Kentab A, Repetto GM, Hashem M, Alkuraya FS (2012) Genomic analysis of mitochondrial diseases in a consanguineous population reveals novel candidate disease genes. J Med Genet 49:234–241

Smeitink J, van den Heuvel L, DiMauro S (2001) The genetics and pathology of oxidative phosphorylation. Nat Rev Genet 2:342–352

Smith LL, Beggs AH, Gupta VA (2013) Analysis of skeletal muscle defects in larval zebrafish by birefringence and touch-evoke escape response assays. J Vis Exp JoVE e50925–e50925

Vasta V, Ng SB, Turner EH, Shendure J, Hahn SH (2009) Next generation sequence analysis for mitochondrial disorders. Genome Med 1:100

Wang Y, Tajkhorshid E (2008) Electrostatic funneling of substrate in mitochondrial inner membrane carriers. Proc Natl Acad Sci USA 105:9598–9603. doi:10.1073/pnas.0801786105

Westerfield M (2007) The Zebrafish Book: a guide for the laboratory use of Zebrafish (Danio Rerio)

Wolf NI, Smeitink JA (2002) Mitochondrial disorders A proposal for consensus diagnostic criteria in infants and children. Neurology 59:1402–1405

Zallot R, Agrimi G, Lerma-Ortiz C, Teresinski HJ, Frelin O, Ellens KW, Castegna A, Russo A, de Crécy-Lagard V, Mullen RT (2013) Identification of mitochondrial coenzyme A transporters from maize and Arabidopsis. Plant Physiol 162:581–588